Short communication

High efficient electrooxidation of formic acid at a novel Pt–indole composite catalyst prepared by electrochemical self-assembly

Weiqiang Zhou [a,c], Chuanyi Wang [b], Jingkun Xu [a,*], Yukou Du [c,*], Ping Yang [c]

[a] *Jiangxi Key Laboratory of Organic Chemistry, Jiangxi Science and Technology Normal University, Nanchang 330013, PR China*
[b] *Xinjiang Technical Institute of Physics & Chemistry, Chinese Academy of Sciences, Urumqi 830011, PR China*
[c] *College of Chemistry, Chemical Engineering and Materials Science, Soochow University, Suzhou 215123, PR China*

ARTICLE INFO

ABSTRACT

Self-assembly of Pt and indole into a novel composite catalyst on a glassy carbon electrode (GC) has been developed by a one-step electrodeposition in the presence of 3.0 mM H_2PtCl_6 and 0.1 mM indole. Compared to Pt/GC and Pt/C, the novel Pt–indole composite catalyst exhibits higher catalytic activity and stronger poisoning tolerance for electrooxidation of formic acid. The adsorption strength of CO on the prepared Pt–indole composite catalyst is greatly weakened as demonstrated by CO stripping voltammograms. Because of its advantageous catalytic activity and poisoning tolerance, the novel Pt–indole composite catalyst is anticipated to find interesting applications in many important fields such as energy and catalysis.

1. Introduction

Direct formic acid fuel cell has attracted great attention because formic acid is of nontoxicity and has low crossover, as compared to methanol [1]. The electrooxidation of formic acid at traditional Pt catalyst is proposed to follow a dual-pathway mechanism [2–9]: one is through dehydrogenation to form CO_2 and the other is through dehydration to form an intermediate product such as CO_{ad}, which is a source of poisoning. In order to mitigate the CO_{ad}-like poisoning, an ideal approach is to redirect the reaction from the intermediate pathway to the direct pathway. In this context, derivative Pt catalysts were developed through modifications, such as Pt modified with other noble metals (i.e., to form so-called bimetallic catalysts), with Fe-macrocycle compounds, or with manganese oxide single crystalline nanorods [10–16]. Enhanced activities for the direct oxidation of formic acid were observed with these modified Pt catalysts. However, the modifications were usually accomplished at the expense of complicated preparation processes and costly materials.

Due to the interaction between Pt and indole, simply soaking pre-electrodeposited Pt particles in solutions of indole can promote the direct electrooxidation of formic acid to some extent [17]. However, the pre-electrodeposited Pt particles have a small surface area, and thus no appreciable amount of indole could be adsorbed. Currently, various hybrid thin films with improved properties have been prepared by electrochemical self-assembly of inorganic compound films in the presence of certain organic molecules [18]. In view of indole containing an N–H group which promotes efficient adsorption on Pt surface, electrochemical self-assembly to form Pt–indole composite catalyst should be achievable. In the present work, we report a one-step preparation of novel Pt–indole composite catalyst by the electrochemical self-assembly method. The new promoter, indole, is found to be very effective in inhibiting self-poisoning, thus to improve the catalytic activity for the electrooxidation of formic acid.

2. Experimental

2.1. Materials and apparatus

Indole (In, analytical-grade, Shandong Pingyuan Hengyuan Chemical Co., Ltd., China), H_2PtCl_6 (Shanghai Shiyi Chemicals Reagent Co., Ltd., China), JM 20 wt.% Pt/C powders (Johnson Matthey), and 5 wt.% Nafion solution (DuPont) were used as received. Formic acid was of analytical-grade. Doubly distilled water was used throughout the work. The electrochemical experiments were carried out using a CHI 660B potentiostat/galvanostat (Shanghai Chenhua Instrumental Co., Ltd., China) at room temperature. A glassy carbon electrode (GC, 3 mm diameter) was used as the substrate electrode. The counter electrode and the reference
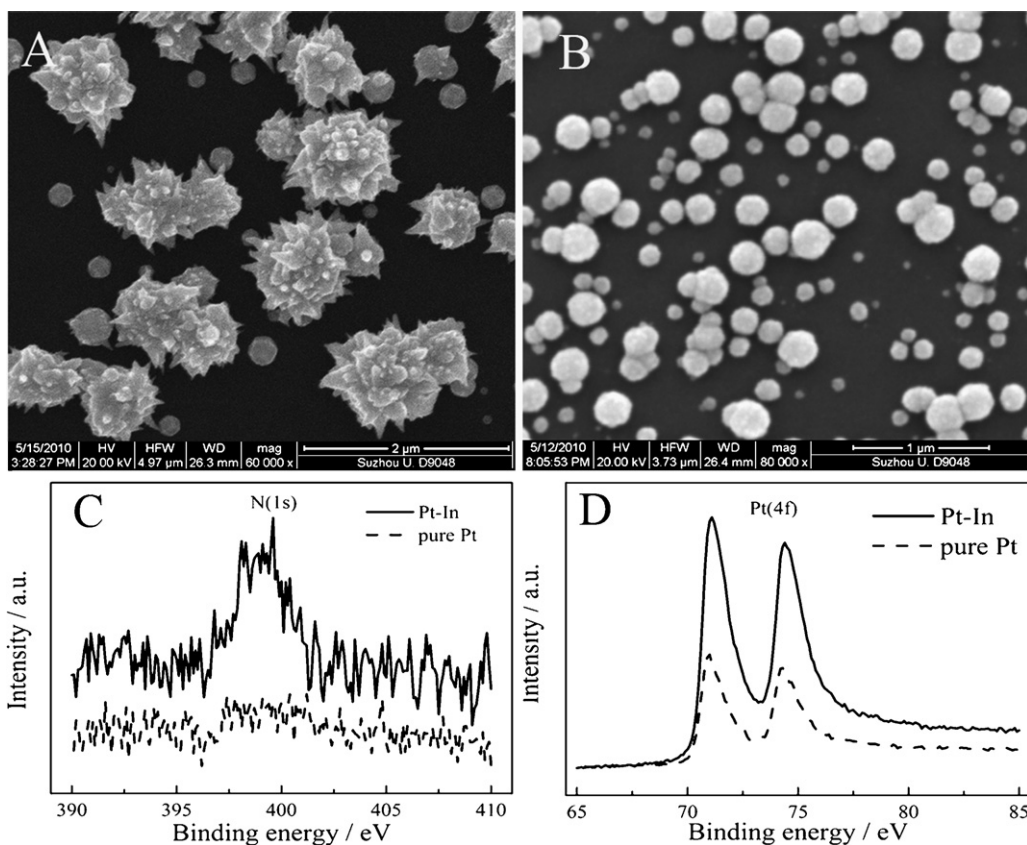
Fig. 1. SEM micrographs of Pt/GC (A) and Pt–In/GC (B); XPS of N(1s) (C) and Pt(4f) (D) from pure Pt and Pt–In.

were Pt wire and saturated calomel electrode (SCE), respectively. Electrolyte solutions were deaerated by a dry nitrogen stream and kept with a slight overpressure of nitrogen during the experiments. A scanning electron microscope (SEM, FEI Quanta 200) was used for morphology studies. Surface composition of prepared composite catalysts was examined by X-ray photoelectron spectroscopy (XPS) recorded on a KRATOS Analytical X-ray photoelectron spectrometer.

2.2. Electrode preparation

Before modification, GC surface was polished with a 0.3 μm alumina slurry, and then rinsed with doubly distilled water in an ultrasonic bath. Pt–indole composite catalyst on GC (defined as Pt–In/GC) was fabricated by electrochemical self-assembly in the presence of 3.0 mM H_2PtCl_6 + 0.1 M KCl + 0.1 mM indole at −0.2 V. As indole was inert at −0.2 V, no electropolymerization of indole occurred under the present condition; due to its function group N–H, indole only adsorbed on the surface of Pt during the electrodeposition. The amount of deposited Pt was determined by the integrated charges during electrodeposition, with an assumption of a 100% current efficiency [19]. For comparison, Pt/GC (i.e., Pt deposited on GC), JM Pt/C and In/GC were also prepared. Pt/GC was obtained by a similar method as stated above, i.e., electrodeposition in a solution consisting of 3.0 mM H_2PtCl_6 and 0.1 M KCl. For JM Pt/C electrode, JM 20 wt.% Pt/C powders (3.5 mg) were dispersed in Nafion ethanol solution (1.0 mL) under ultrasonic stirring. After that, the catalyst ink (12 μL) was dropped by injector onto the surface of GC and dried in air. In/GC electrode was obtained via controlling indole coverage on part of GC surface by a dripping method. In this paper, the amount of Pt in all cases was controlled as 8.4 μg.

3. Results and discussion

Pt particles were easily prepared by potentiostatic methods, which adhered strongly to GC. The morphologies of Pt particles obtained from different electrolytes have been characterized by SEM (Fig. 1A and B). Irregular Pt particles were produced by electrodeposition in the presence of 3.0 mM H_2PtCl_6 and 0.1 M KCl (Fig. 1A). However, smaller Pt nanoparticles (on average) were obtained when indole monomers were added into the system (Fig. 1B). The decrease in the particle size may be resulted from that indole functions as a protectant which inhibits Pt particles from growing up. On the other hand, similar to the case of electrochemical self-assembly previously reported by Yoshida et al. [18], the adsorption of indoles occurred simultaneously with the Pt growing, thus forming composites consisting both of Pt and indole.

Fig. 1C and D shows the XPS of N(1s) and Pt(4f) of pure Pt and Pt–In samples, respectively. The peak of N(1s) from the Pt–In sample illustrates that indole has adsorbed on the Pt surface. In Fig. 1D, the two peaks of Pt(4f) at 70.9 and 74.2 eV from the pure Pt sample are identified as 4f7/2 and 4f5/2, respectively, which are consistent with previous studies [20]. However, increased binding energies of Pt from Pt–In are observed; the 4f7/2 and 4f5/2 doublets locate at 71.1 and 74.4 eV, respectively. A small increase in Pt binding energies has also been observed in Pt–Pb [21] and Pt–Bi [22]. The increase in the binding energies of Pt indicates the presence of a certain degree of interactions of indole molecules with the Pt surface.

Representative cyclic voltammograms (CVs) of Pt–In/GC, Pt/GC and In/GC were recorded in the presence of 0.5 M H_2SO_4 solution (Fig. 2A). Different responses to hydrogen adsorption/desorption on Pt–In/GC and Pt/GC are noticed in the potential region
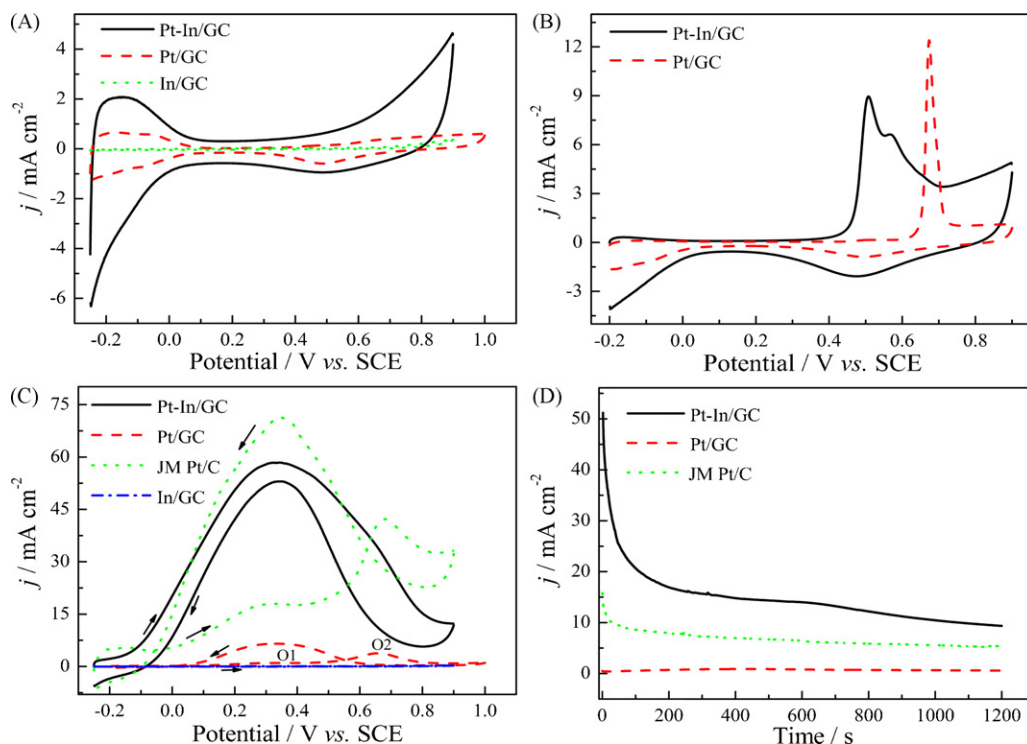
Fig. 2. (A) CVs of Pt–In/GC, Pt/GC and In/GC in a 0.5 M H$_2$SO$_4$ solution at 50 mV s^{-1}; (B) CO stripping voltammograms obtained on Pt–In/GC and Pt/GC in a 0.5 M H$_2$SO$_4$ solution at 50 mV s^{-1}; (C) CVs of formic acid oxidation at Pt–In/GC, Pt/GC, JM Pt/C and In/GC in the presence of 0.5 M formic acid and 0.5 M H$_2$SO$_4$ at 50 mV s^{-1}; (D) chronoamperometic curves of formic acid oxidation at Pt–In/GC, Pt/GC and JM Pt/C in the presence of 0.5 M formic acid and 0.5 M H$_2$SO$_4$ at 0.2 V.

between −0.25 and 0.1 V. For Pt–In/GC, the hydrogen desorption peak possesses a hump, and the current densities of hydrogen adsorption/desorption peaks are increased largely. Note that the background current originated from In/GC is negligible in the potential region between −0.25 and 0.1 V (c.f. Fig. 2A). Therefore, according to the work done by Liu et al. [23], the integrated charges (Q_H) in the hydrogen desorption region for Pt–In/GC and Pt/GC are 0.71 and 0.23 mC cm^{-2}, respectively; and the electrochemical active surface areas (EASAs) of Pt–In/GC and Pt/GC are 2.82 and 0.91 m^2 g^{-1}, respectively. This suggests that Pt–In/GC possesses a much higher active surface area than Pt/GC at the same Pt loading. Combining with the SEM observations (Fig. 1A and B), we can tentatively conclude that the presence of indole molecules in the electrolyte solution favors the formation of small Pt particles, leading to an increase in the density of active sites on the electrode surface.

In order to test the poisoning effect of CO on different electrodes, irreversible CO$_{ad}$ layer was formed by exposing both Pt–In/GC and Pt/GC to a CO-saturated 0.5 M H$_2$SO$_4$ solution for 30 min. Fig. 2B shows the stripping voltammograms of CO at Pt–In/GC and Pt/GC in 0.5 M H$_2$SO$_4$. As seen from Fig. 2B, significant differences in the onset potential (E_{onset}) and peak potential (E_{peak}) for CO electrooxidation at Pt–In/GC and Pt/GC are observed. At Pt–In/GC, the E_{onset} and E_{peak} are 0.38 and 0.51 V, respectively, which are much lower than those at Pt/GC (E_{onset} = 0.63 V and E_{peak} = 0.67 V). The negative shift in the E_{onset} and E_{peak} of the CO electrooxidation implies that CO is more easily oxidized at Pt–In/GC than at Pt/GC. In addition, there is a shoulder-like peak at Pt–In/GC, which is mainly due to the modification of Pt surface microstructure by indole adsorption. It has been reported that the stripping voltammograms of CO at different crystal planes Pt are different [24–26]. The above results indicate that compositing of Pt with indole (i.e., Pt–In/GC) is beneficial to the electrooxidation of small organic molecules (such as formic acid, methanol and ethanol). To confirm this, parallel stud-

ies on electrocatalytic activities of Pt–In/GC, Pt/GC and commercial JM Pt/C were conducted by CV measurements.

Fig. 2C shows the CVs of formic acid oxidation at Pt–In/GC, Pt/GC and JM Pt/C in a solution of 0.5 M formic acid + 0.5 M H$_2$SO$_4$. As seen from Fig. 2C, Pt/GC exhibits the regular characteristics of formic acid oxidation at a Pt electrode, which follows the dual-pathway mechanism [2–9]. A weak anodic peak (O$_1$, 0.97 mA cm^{-2}) at 0.37 V is attributed to the direct oxidation of formic acid via dehydrogenation pathway; while the second large anodic peak (O$_2$, 3.46 mA cm^{-2}) at 0.66 V is related to the dehydration of formic acid [2]. The ratio of the two peak current densities (j_{O1}/j_{O2}) is 0.28, indicating that the electrooxidation of formic acid at Pt/GC occurs mainly through the dehydration pathway [13]. Similar to the case of Pt/GC, the electrooxidation of formic acid at JM Pt/C was also mainly through the dehydration pathway, where the first peak current density at 0.33 V is 18.0 mA cm^{-2}, the second peak current density at 0.67 V is 42.13 mA cm^{-2}, and the ratio of the two current densities is 0.43. However, the CV of Pt–In/GC is dramatically different from those of Pt/GC and JM Pt/C. First, at Pt–In/GC, the onset oxidation potential of formic acid is shifted negatively to −0.20 V, which means that formic acid is much easier to be oxidized compared to the former two cases. Second, the only anodic peak at 0.34 V is well defined and enhanced significantly (58.54 mA cm^{-2}); the ratio of the current densities at 0.34 and 0.66 V reaches to 1.76, which is much higher than that of 0.28 for Pt/GC. The high ratio of j_{O1}/j_{O2} represents the enhancement of the direct oxidation pathway [13]. Therefore, the electrooxidation of formic acid at Pt–In/GC is mainly through the direct oxidation pathway, and thus less poisonous intermediate is produced. Moreover, the first peak current density at Pt–In/GC is about 60 and 3.25 times of those at Pt/GC and JM Pt/C, respectively. This demonstrates that the electrocatalytic oxidation of formic acid at Pt is greatly enhanced by the presence of indole molecules. A tentative mechanism for the enhanced performance is proposed as the following: (1) Indole with an N–H group
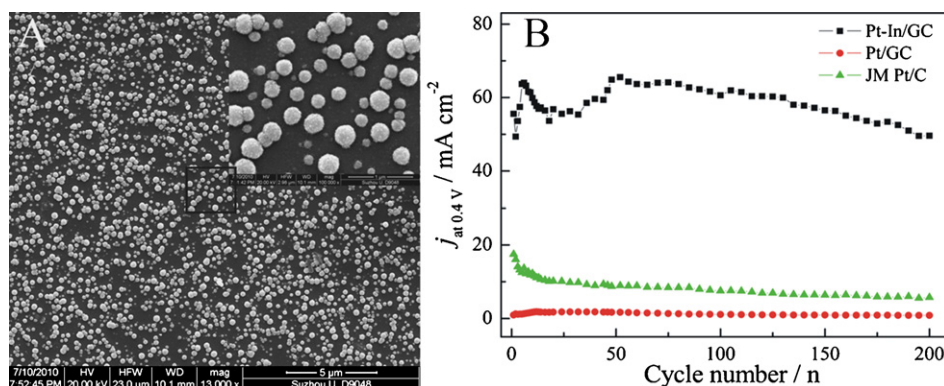
Fig. 3. (A) SEM micrograph of Pt–indole electrode polarized at 0.2 V after 1200s, inset is at a higher magnification and (B) the current densities of formic acid oxidation at Pt–In/GC, Pt/GC and JM Pt/C as a function of CV cycle numbers in the presence of 0.5 M formic acid and 0.5 M H_2SO_4 at 0.4 V.

prefers to adsorb on Pt surface. The surface of Pt will be divided into a lot of small grids framed with indole molecules due to the nature of selective adsorption. The electrooxidation of formic acid occurs on the surface of those small grids uncovered by indole molecules. Dehydration reaction, which generated the poisoning intermediate CO_{ad}, is strongly dependent on the surface microstructure of Pt [27,28]. The adsorbed indole on Pt surface will modify the Pt surface microstructure and block some sites of Pt, which could be active in the dehydration reaction, and consequently the formation of CO_{ad} is inhibited. As the CO pathway is inhibited, the direct pathway becomes possible; (2) It has been reported that the adatoms on Pt surface such as Pb, Bi, Sb and macrocycle compounds functioned as electron donors to the surface of Pt, facilitating the direct oxidation of formic acid [15,29–31]. Likewise, indole with an abundant amount of electrons will generate an electronic effect when it adsorbs onto the Pt surface. As observed by XPS (c.f. Fig. 1D), the small increase in Pt binding energies for Pt–indole catalyst supports that indole can affect the electron distribution on the Pt surface, and thus changes the reaction pathway of formic acid electrooxidation.

The stabilities of the catalysts were evaluated at 0.2 V for a period of 1200s. Fig. 2D shows the chronoamperometric curves of formic acid oxidation at Pt–In/GC, Pt/GC and JM Pt/C. As observed from Fig. 2D, formic acid oxidation at Pt–In/GC gives the highest oxidation current density. At the end of the test, the oxidation current densities at Pt–In/GC, Pt/GC and JM Pt/C are 9.37, 0.58 and 5.37 mA cm^{-2}, respectively, which demonstrates that the electrocatalytic stability of Pt–In/GC for formic acid oxidation is much better than those of Pt/GC and JM Pt/C. Additionally, SEM characterization of Pt–indole electrode polarized at 0.2 V after 1200s has been conducted (Fig. 3A). As seen from Fig. 3A, the Pt–indole catalysts are stable on GC.

In practice, a long-period of stability of an electrode is crucial. From this prospect, CVs of 200 cycles for Pt–In/GC, Pt/GC and JM Pt/C were examined in the presence of 0.5 M formic acid + 0.5 M H_2SO_4 at 50 mV s^{-1}. Fig. 3B shows the anodic current densities of formic acid oxidation at 0.4 V during a total of 200 cycles. For Pt–In/GC, the current density approaches a maximum of 65.54 mA cm^{-2} at the 52nd cycle, and then decreases to 49.58 mA cm^{-2} at the 200th cycle, with a total decrease of 24.35% relative to the current maximum. For Pt/GC electrode, however, the current density reaches its maximum (1.80 mA cm^{-2}) at the 12th cycle, and then decreases to 0.83 mA cm^{-2} at the 200th cycle, with a total decrease of 53.89% relative to the maximum. For JM Pt/C, the current density decreases gradually from 17.5 to 5.72 mA cm^{-2} with a total decrease of 67.3%. These observations clearly support the fact that Pt–In/GC has much higher catalytic activity and better stability for formic acid oxidation than Pt/GC and JM Pt/C.

4. Conclusions

A novel Pt–indole composite catalyst has been prepared by a simple electrochemical self-assembly method. This study demonstrates that Pt–indole shows superior performance in both aspects of electrocatalytic activity and stability towards the oxidation of formic acid. In addition, the results of CO stripping voltammograms support the fact that the adsorption strength of CO on Pt–indole catalyst is greatly weakened. Because of its simple preparation and superior performance, the novel Pt–indole composite catalyst is expected to find important applications in many practical fields such as electrode materials, fuel cells, and catalysts.

Acknowledgements

References

[1] C. Rice, S. Ha, R.I. Masel, P. Waszczuk, A. Wieckowski, T. Barnard, J. Power Sources 111 (2002) 83–89.
[2] A. Capon, R. Parsons, J. Electroanal. Chem. 45 (1973) 205–231.
[3] G.Q. Lu, A. Crown, A. Wieckowski, J. Phys. Chem. B 103 (1999) 9700–9711.
[4] R.S. Jayashree, J.S. Spendelow, J. Yeom, C. Rastogi, M.A. Shannon, P.J.A. Kenis, Electrochim. Acta 50 (2005) 4674–4682.
[5] X. Wang, J.M. Hu, I.M. Hsing, J. Electroanal. Chem. 562 (2004) 73–80.
[6] V. Selvaraj, A.N. Grace, M. Alagar, J. Colloid Interface Sci. 333 (2009) 254–262.
[7] V. Selvaraj, M. Alagar, K.S. Kumar, Appl. Catal. B: Environ. 75 (2007) 129–138.
[8] Z.Z. Zhu, Z. Wang, H.L. Li, Appl. Surf. Sci. 254 (2008) 2934–2940.
[9] J.H. Choi, K.J. Jeong, Y. Dong, J. Hanb, T.H. Lim, J.S. Lee, Y.E. Sungc, J. Power Sources 163 (2006) 71–75.
[10] B. Peng, J.Y. Wang, H.X. Zhang, Y.H. Lin, W.B. Cai, Electrochem. Commun. 11 (2009) 831–833.
[11] S. Uhm, S.T. Chung, J. Lee, Electrochem. Commun. 9 (2007) 2027–2031.
[12] N. Kristian, Y.S. Yan, X. Wang, Chem. Commun. (2008) 353–355.
[13] M.S. El-Deab, L.A. Kibler, D.M. Kolb, Electrochem. Commun. 11 (2009) 776–778.
[14] X.C. Zhou, W. Xing, C.P. Liu, T.H. Lu, Electrochem. Commun. 9 (2007) 1469–1473.
[15] X.C. Zhou, C.P. Liu, J.H. Liao, T.H. Lu, W. Xing, J. Power Sources 179 (2008) 481–488.
[16] Z.H. Zhang, X.C. Zhou, C.P. Liu, W. Xing, Electrochem. Commun. 10 (2008) 131–135.
[17] W.Q. Zhou, Y.K. Du, H.M. Zhang, J.K. Xu, P. Yang, Electrochim. Acta 55 (2010) 2911–2917.
[18] T. Yoshida, K. Miyamoto, N. Hibi, T. Sugiura, H. Minoura, D. Schlettwein, T. Oekermann, G. Schneider, D. Wöhrle, Chem. Lett. 27 (1998) 599–600.
[19] C.W. Kuo, L.M. Huang, T.C. Wen, A. Gopalan, J. Power Sources 160 (2006) 65–72.
[20] J.P. Wang, P. Holt-Hindle, D. MacDonald, D.F. Thomas, A. Chen, Electrochim. Acta 53 (2008) 6944–6952.
[21] D.R. Blasini, D. Rochefort, E. Fachini, L.R. Alden, F.J. DiSalvo, C.R. Cabrera, H.D. Abruña, Surf. Sci. 600 (2006) 2670–2680.

[22] S.J. Kang, J. Lee, J.K. Lee, S.Y. Chung, Y. Tak, J. Phys. Chem. B 110 (2006) 7270–7274.
[23] Z.L. Liu, J.Y. Lee, M. Han, W.X. Chen, L.M. Gan, J. Mater. Chem. 12 (2002) 2453–2458.
[24] A. Cuesta, A. Couto, A. Rincón, M.C. Pérez, A. López-Cudero, C. Gutiérrez, J. Electroanal. Chem. 586 (2006) 184–195.
[25] A. López-Cudero, A. Cuesta, C. Gutiérrez, J. Electroanal. Chem. 579 (2005) 1–12.
[26] A. López-Cudero, A. Cuesta, C. Gutiérrez, J. Electroanal. Chem. 586 (2006) 204–216.
[27] J. Clavilier, S.G. Sun, J. Electroanal. Chem. 199 (1986) 471–480.
[28] T. Iwasita, X.H. Xia, E. Herrero, H.D. Liess, Langmuir 12 (1996) 4260–4265.
[29] V. Climent, E. Herrero, J.M. Feliu, Electrochim. Acta 44 (1998) 1403–1414.
[30] A.C. Luna, T. Iwasita, V. Vielstich, J. Electroanal. Chem. 196 (1985) 301–314.
[31] M.D. Maciá, E. Herrero, J.M. Feliu, J. Electroanal. Chem. 554 (2003) 25–34.